Probing Ground-to-CT State Electronic Coupling for the System with No Apparent Charge Transfer Absorption Intensity by Ultrafast Visible-Pump/Mid-IR-Probe Spectroscopy

ARTICLE *in* THE JOURNAL OF PHYSICAL CHEMISTRY C · OCTOBER 2011

Impact Factor: 4.77 · DOI: 10.1021/jp207122e

6 AUTHORS, INCLUDING:

Youn K. Kang
Sangmyung University
34 PUBLICATIONS **608** CITATIONS

SEE PROFILE

THE JOURNAL OF PHYSICAL CHEMISTRY C

ARTICLE

pubs.acs.org/JPCC

Probing Ground-to-CT State Electronic Coupling for the System with No Apparent Charge Transfer Absorption Intensity by Ultrafast Visible-Pump/Mid-IR-Probe Spectroscopy

Hyeong-Mook Kim,[†] Jaeheung Park,[‡] Young Tak Lee,[†] Manho Lim,[*,‡] Young Keun Chung,[*,†] and Youn K. Kang[*,§]

[†]Intelligent Textile System Research Center, Department of Chemistry, College of Natural Sciences, Seoul National University, Seoul, 151-747, Korea

[‡]Department of Chemistry and Chemistry Institute of Functional Materials, Pusan National University, Busan, 609-735, Korea

[§]Department of Chemistry, Sangmyung University, Seoul 110-743, Korea

Supporting Information

ABSTRACT: New π-stacked $[Ru(tpy)_2]^{2+}$ (**T_T**)-benzoquinone (Q) donor−acceptor (D−A) systems, [Ru(6-(2-cyclohexa-2′,5′-diene-1,4-dione)-2,2′:6′,2″-terpyridine)(2,2′:6′,2″-terpyridine)][PF_6]$_2$ (**TQ_T**), and [Ru(6-(2-cyclohexa-2′,5′-diene-1,4-dione)-2,2′:6′,2″-terpyridine)(4′-phenyl-2,2′:6′,2″-terpyridine)][PF_6]$_2$ (**TQ_TPh**) have been synthesized and characterized. Orthogonal alignment of Q to the tpy ligand imposes this unit juxtaposed cofacially on the central pyridyl ring in another tpy with a typical van der Waals distance. The low-energy electronic absorptions of these complexes are mainly metal-to-ligand charge transfer (MLCT) in nature, similar to that observed in **T_T** benchmark system, and do not exhibit distinguishable metal-to-Q charge transfer (MQCT) absorption in spite of the proximal location of the electron acceptor unit (Q) to the electron donor unit (**T_T**). TD-DFT calculation supports the experimental results that the collective oscillator strength of MQCT bands remains ∼0.002. Due to the negligible intensity of MQCT bands, evaluation of H_{DA} between the ground and the lowest energy MQCT states are not available through conventional Mulliken−Hush analysis. For such systems, H_{DA} values were successfully evaluated from the relative difference (ξ) of the carbonyl stretching frequency between the neutral Q and its one-electron radical anion, which was determined by an ultrafast visible-pump/mid-IR-probe (TrIR) spectroscopic method. TrIR results showed that the partial charge localized on the Q moiety in the MQCT state was ca. −0.97*e*, and the corresponding H_{DA} was ∼1600 cm^{-1}. This value was in good agreement with that estimated by the Mulliken population analysis of the ground-state geometry.

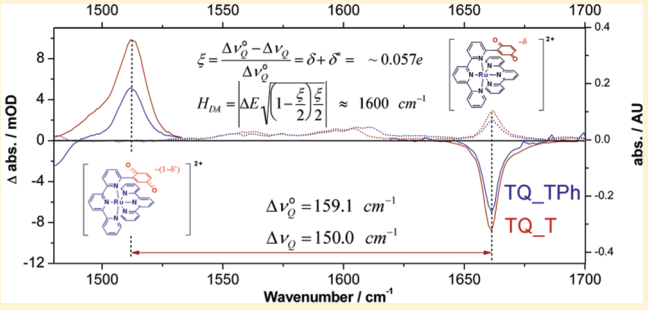

The theoretical background to quantify an electronic coupling matrix element (H_{DA}) between the ground and the charge transfer (CT) states by optical CT absorption intensity had been first established by Mulliken and Hush and later expanded on by a number of scientists.[1−4] While close evaluation of H_{DA} by either an experimentally determined transition dipole moment (μ) of a CT absorption band[5−18] or a pure computational calculation through generalized Mulliken−Hush analysis[19−22] was made possible, Rubtsov et al. reported[23] an interesting result that provides a protocol to determine H_{DA} by a femtosecond visible-pump/mid-IR-probe spectroscopy (TrIR).

If adiabatic ground (Ψ_G) and CT (Ψ_{CT}) state wave functions are expressed as the following equations[24]

$$\Psi_G = C_1\psi_1 + C_2\psi_2 \quad (1a)$$

$$\Psi_{CT} = C_1\psi_2 - C_2\psi_1 \quad (1b)$$

where ψ_1 and ψ_2 are wave functions of zero-order ground and CT states,[4] respectively, a first-order perturbation theory[4] predicts that

$$|C_1C_2| = |H_{DA}/\Delta E| \quad (2)$$

where ΔE is the ground-to-CS state energy gap. As the interaction between ψ_1 and ψ_2 increases, the magnitude of C_2 increases; the degree of CT character in the ground state or that of ground-state character in the CT state scales with C_2^2. For a D−A molecule where A is Q, the vibrational frequency shift of the carbonyl stretching mode in the CT state relative to that in the ground state ($\Delta\nu_Q$) depends on the charge built into the Q moiety. The linear correlation between $\Delta\nu_Q$ and the degree of

Received: July 26, 2011
Revised: September 30, 2011
Published: October 01, 2011

Chart 1. Structures of $[Ru(tpy)_2]^{2+}$−Q (TQ_T) and $[Ru(tpy)(tpyPh)]^{2+}$−Q (TQ_TPh) along with $[Ru(tpy)_2]^{2+}$ (T_T)

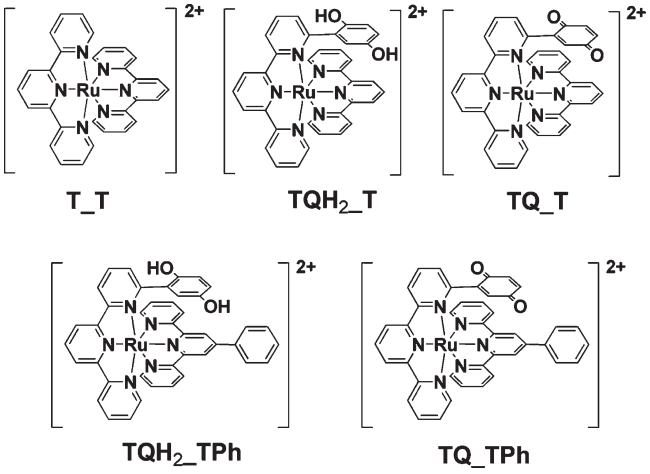

charge built on the corresponding radical anion has been determined empirically by Rubtsov et al.[23] as $\xi \approx 2C_2^2$, where $\xi = (\Delta\nu_Q^\circ - \Delta\nu_Q)/\Delta\nu_Q^\circ$ and $\Delta\nu_Q^\circ$ is the $\Delta\nu_Q$ of the system with no D−A interaction.[6,25] From this relation along with eq 2, H_{DA} can be recast in the form of eq 3 and becomes available if two parameters, ξ and ΔE, are known.

$$H_{DA} = \left|\Delta E\sqrt{\left(1-\frac{\xi}{2}\right)\frac{\xi}{2}}\right| \quad (3)$$

ξ can be obtained by TrIR with proper $\Delta\nu_a^\circ$ and ΔE values; $\Delta\nu_a^\circ$ can be determined by measuring the vibational frequency difference between the ground (ν_a°) and the reduced state ($\nu_a^{-\circ}$) of the electron acceptor, while ΔE can be obtained by conventional electrochemical methods.[26]

While Mulliken−Hush analysis has been a widely accepted protocol for evaluation of H_{DA}, its application to a variety of real systems is limited because the CT absorption band is only observable when H_{DA} is sufficiently large to reach or surpass a perturbation limit in most real systems, although the Mulliken−Hush relation is assumed to be valid only in the weak coupling limit.[4,8,16] Moreover, even if a CT absorption band is available, an accurate quantification of H_{DA} is often obscured by interference when the CT state overlaps energetically with other states or there is a significant degree of mixing between the CT state and others. Therefore, evaluation of H_{DA} by eq 2 through the TrIR approach is particularly useful for a system that does not exhibit distinguishable CT absorption.

During our ongoing effort to develop a Ru-based chromophore system that absorbs light over a wide range of the energy window, we newly synthesized [Ru(6-(2-cyclohexa-2′,5′-diene-1,4-dione)-2,2′:6′,2″-terpyridine)(2,2′:6′,2″-terpyridine)][PF_6]$_2$ (**TQ_T**) and [Ru(6-(2-cyclohexa-2′,5′-diene-1,4-dione)-2,2′:6′,2″-terpyridine)(4′-phenyl-2,2′:6′,2″-terpyridine)][PF_6]$_2$ (**TQ_TPh**), in which a benzoquinone (Q) electron acceptor is located on top of the central pyridyl ring of a tpy ligand in a juxtaposed manner (Chart 1). The proximal location of the electron acceptor near the electron donor Ru metal was expected to give rise to an orbital interaction between the Ru-centered HOMO and the Q-centered LUMO, which might generate a metal-to-Q CT (MQCT) band in the lower energy region relative to the already existing metal-to-tpy CT band (MLCT). This feature would facilitate light harvesting over a wide range of the energy window. Contrary to our anticipation, however, the absorption spectra of **TQ_T** and **TQ_TPh** complexes resembled those of a **T_T** archetype exhibiting only conventional MLCT bands. The MQCT absorption did not prevail. The mere absence of a MQCT absorption band is not surprising if ground-to-MQCT H_{DA} is not large.[27−29] Interestingly, however, further investigation by the TrIR spectroscopic method revealed that the H_{DA} was nonetheless substantial. Here, we report the details of these results, which clearly demonstrate the usefulness of TrIR in determining the magnitude of H_{DA} where the CT absorption intensity is negligible.

The **TQ_T** and **TQ_TPh** complexes were synthesized by a conventional synthetic protocol, which is summarized in Scheme S1, Supporting Information. These complexes were fully characterized by a series of 1D and 2D NMR studies, high-resolution mass spectroscopy, and electronic and vibrational spectroscopies. Optimized geometries by DFT calculation at the B3LYP/6-31g(d)-LANL2DZ level show that the Q plane is orthogonally attached to the 6-position of one tpy ligand and is nearly coplanar with a juxtaposed pyridyl ring plane in another tpy ligand for both **TQ_T** and **TQ_TPh**. Ru-to-Q centroid distances are 4.69 and 4.72 Å for **TQ_T** and **TQ_TPh**, respectively (Figure 1). Q plane-to-pyridyl plane distances are 3.58 and 3.51 Å, respectively, indicating that the Q and pyridyl ring planes are in the typical van der Waals distance for both **TQ_T** and **TQ_TPh**. Due to this π stacking, ^{1}H NMR peaks corresponding to quinonyl protons appear at 5.56, 6.41, and 6.68 ppm for **TQ_T** and 5.63, 6.45, and 6.52 for **TQ_TPh**, which are ∼1 ppm upfield shifted relative to those of a conventional Q. However, the degree of compression between Q and tpy is only moderate compared to that of the cofacially aligned porphyrin−Q system reported previously by the Therien group.[50,51] The optimized geometry of **TQ_TPh** shows that the dihedral angle between the peripheral phenyl substituent at the 4′-position and the central pyridyl ring is ∼36°.

The electrochemical redox potentials of the two complexes in acetonitrile were recorded, and their values are listed in Table 1. Both complexes exhibit one-electron reversible oxidation at 1.64 and 1.62 V and one-electron reversible reduction at −0.02 and 0.01 V for **TQ_T** and **TQ_TPh**, respectively.[52] The energies and 3-dimensional isosurfaces of the frontier MOs of **TQ_T** (Figure S1 and Table S1, Supporting Information) obtained by DFT calculation show that the HOMO is mainly localized in the Ru metal (74.6%) while the LUMO is in Q (93.2%). In the case of **TQ_TPh**, however, the electronic population in HOMO is delocalized over the phenyl-tpy ligand (50.6%) as well as the Ru metal (42.5%) while that in LUMO is localized in Q (93.3%). Consequently, the energy level of HOMO in **TQ_TPh** was significantly destabilized by 0.43 eV relative to that in **TQ_T**. This calculation result is, however, obviously contradictory to the experimental results. The oxidation potentials of two complexes measured by cyclic voltammetry were nearly identical to each other. This discrepancy might be due to the overemphasized coplanarity in the calculated structure. The optimized geometry of **TQ_TPh** shows that the dihedral angle between the peripheral phenyl substituent at the 4′-position of the tpy ligand and the central pyridyl ring was only ∼36°. In solution phase, the electronic delocalization effect should decrease due to the rotational degree of freedom. Single-point calculation with

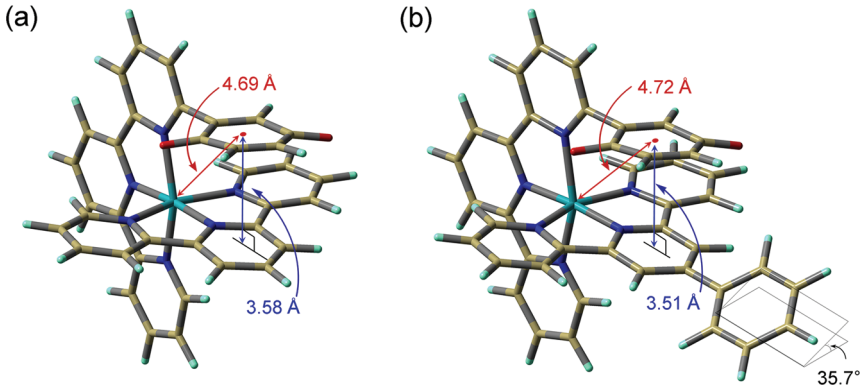

Figure 1. Geometries of **TQ_T** (a) and **TQ_TPh** (b). Metal-to-quinonyl plane centroid distances are shown in red. Quinonyl plane-to-pyridyl plane distances are shown in blue.

Table 1. Spectroscopic and Voltammetric Data

complex	λ_{max}[a] (nm)	λ_{max}[a] (cm^{-1})	$\varepsilon \times 10^4$ M^{-1} cm^{-1}	ν_{CO} (cm^{-1})	$E_{1/2}^{ox}$[b] (V vs NHE)	$E_{1/2}^{red}$[b] (V vs NHE)
TQH_2_T	472	21 186	1.40			
TQ_T	473	21 142	1.34	1661 ± 0.5	1.64 ± 0.02	−0.02 ± 0.02
TQH_2_TPh	482	20 747	2.06			
TQ_TPh	478	20 921	1.91	1661 ± 0.5	1.62 ± 0.02	0.01 ± 0.02

[a] Experimental conditions: solvent = acetonitrile, temperature = 23 °C. [b] Experimental conditions: [compound] = 5 mM; [$TBAPF_6$] = 0.1 M; solvent = acetonitrile; temperature = 23 °C; scan rate = 50 mV/s; reference electrode = Ag/Ag^+; working electrode = glassy carbon. All potentials are referenced to a ferrocene/ferrocenium redox couple as an internal standard and converted to NHE by the relation ferrocene/ferrocenium vs NHE = +0.64 V.

the orthogonally fixed dihedral angle gives rise to a destabilization of the HOMO of **TQ_TPh** by 0.26 eV, while that with the 30° angle does 0.81 eV, which indicates that the origin of the destabilization of the energy level of HOMO in **TQ_TPh** can be mainly ascribed to electronic delocalization.

It is important to note that the slightly different electronic structures of **TQ_T** and **TQ_TPh** do not manifest in the electronic absorption spectra. The absorption spectra of the two complexes are nearly identical except for the existence of a small shoulder at the ∼520 nm region in the spectrum of **TQ_TPh** (Figure 2a). The absorption spectra of **TQ_T** and **TQH_2_T**, in which Q in **TQ_T** was replaced with hydroquinone (**QH_2**) and thus the CT transition is not allowed, were also virtually identical to each other. Figure 2b shows the normalized electronic absorption profile of the two complexes. These results suggest that both **TQ_T** and **TQ_TPh** exhibit only the MLCT transition without possessing MQCT character. In order to elucidate the nature of the electronic transitions of the absorption spectra further, we performed the TD-DFT calculation. For each complex, we considered 30 singlet excited states. Transitions that have oscillator strengths larger than 0.001 are listed in Table S2, Supporting Information. To compensate for the energy offset between the experimental and the calculation results, 1000 cm^{-1} was equally added to the calculation results and coplotted with the experimentally obtained results (Figure 2b). The calculation result mirrors well the experimental observations. It predicts four ground-to-MQCT transitions (S1−S4 states, Table S2, Supporting Information) for **TQ_T** near 19 000 cm^{-1} with a combined oscillator strength (f) of only 0.0024. The same is true for **TQ_TPh** in that the total f of four predicted ground-to-MQCT transitions is only 0.0015 (S1−S3 and S5 states, Table S2, Supporting Information). It should be noted that the S8 state of **TQ_TPh** has a large 4′-phenylterpyridine-to-Q CT (LQCT) character in addition to MQCT and MLCT characters. The S4 state of **TQ_T** also has such a character, but its oscillator strength is negligible (0.0001) and thus would not contribute to the spectral envelope. The oscillator strength of the S8 state of **TQ_TPh** is, however, 0.0031, which cannot be ignored. The S8 state is a result of mixing among MLCT, LQCT, and MQCT. The electronic transition to this state contributes the shoulder in the spectral envelope near 520 nm, which was noted earlier. Despite the existence of such a band that possesses a high degree of MQCT character, Mulliken−Hush analysis cannot be easily performed because not only is the character of the state the result of a high degree of mixing among different types of transitions but it also overlaps with other states. These results clearly show that MQCT transitions in these complexes are, if any, not available for the Mulliken−Hush analysis, and thus, probing H_{DA} through such an approach is not feasible.

In order to determine the magnitude of H_{DA} between the ground and the MQCT states of these complexes, we attempted to utilize the TrIR method. The ground-state FTIR spectrum in the carbonyl (CO) stretching mode frequency domain of both **TQ_T** and **TQ_TPh** shows a clear absorption band at 1661 cm^{-1} (Figure 3). Upon electronic excitation at 575 nm in which low-energy MLCT tailing or possibly MQCT traces prevail for both **TQ_T** and **TQ_TPh** complexes, the characteristic Q^- mode appeared at 1511 cm^{-1} almost instantly with concomitant bleaching at 1661 cm^{-1} (Table 2, Figure 3). The resulting $\Delta\nu_Q$ value (150 cm^{-1}) is surprisingly similar to that measured in a cofacially aligned porphyrin−Q system (**1a_Zn**) reported by Rubtsov et al.[23] The correlation between transient absorption and bleaching bands was further confirmed by their time-resolved kinetic behaviors (Figure 4). The TrIR decay kinetics of

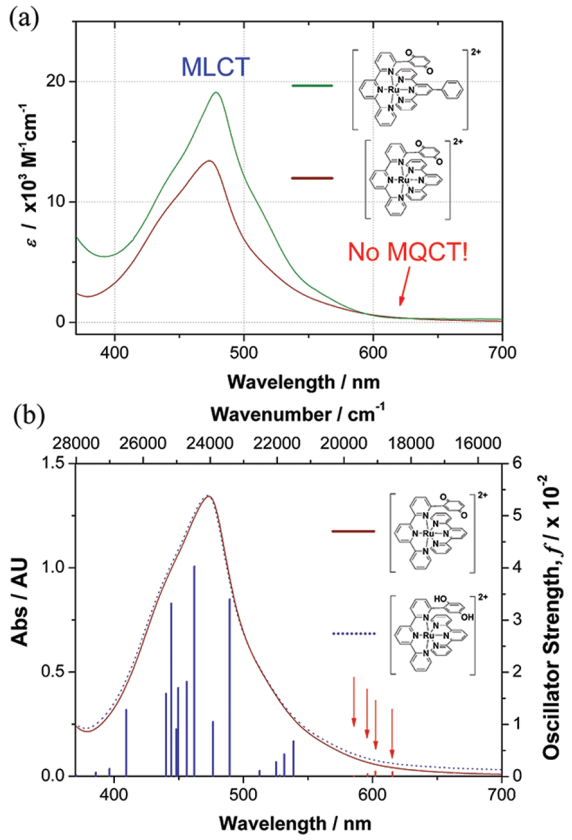

Figure 2. (a) Steady state absorption spectra of **TQ_T** (dark red) and **TQ_TPh** (green) in CH_3CN at 25 °C. (b) Normalized absorption spectra of **TQ_T** (solid red) and its hydroquinone analogue, **TQH_2_T** (dotted blue), in wavelength (bottom abscissa). Calculated transition energies and their corresponding oscillator strengths, *f*, of singlet → singlet transitions by the TD-DFT method are depicted as vertical lines in wavenumbers (top abscissa). Red lines emphasized by red arrows near 600 nm are MQCT transitions. Note that the abscissa on top was shifted by 1000 cm^{-1}.

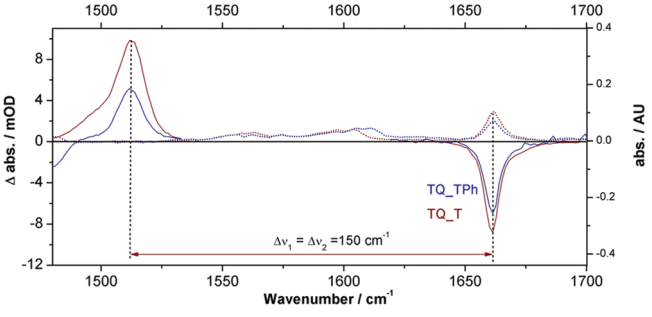

Figure 3. TrIR spectra of **TQ_T** (solid red), **TQ_TPh** (solid blue) at time delays of 1.8 ps. FTIR spectra are shown in dotted lines with corresponding colors. Note that TrIR spectra in the 1530−1620 cm^{-1} region are not shown (experimental conditions: λ_{ex} = 575 nm, solvent = CD_3CN; temp = 23 ± 1 °C).

TQ_T and **TQ_TPh** Q^- modes were fit by a monoexponential function with τ = 22 ± 1 ps for both systems. Those of the Q mode gave τ = 24 ± 2 ps for both, which are in good agreement with Q^- mode kinetics. Therefore, two transient IR bands at 1661 and 1510 cm^{-1} can be unambiguously assigned to the CO stretching mode of ground and CT states, respectively.

Determination of the benchmark reference value of $\Delta\nu_Q^\circ$ is of foremost importance in accurate evaluation of H_{DA}. Although Rubtsov et al. reported $\Delta\nu_Q^\circ$ = 164 cm^{-1} with the cofacially aligned porphyrin−phenylene spacers−Q system, general use of this value appears to be risky because a carbonyl stretching frequency of the one-electron-reduced Q anion radical should be critically dependent on the chemical environment. Even if an absolute value of $\Delta\nu_Q$ in this work is similar to that in their work, it is likely coincidental and thus a simple adoption of $\Delta\nu_Q^\circ$ = 164 cm^{-1} should be avoided.

Clark and Evans reported the IR spectra of the anion radicals of a series of 1,4-benzoquinones.[53] The characteristic carbonyl stretching frequency decreases upon one-electron reduction from neutral quinone to radical anion for six benzoquinones. The degree of frequency shift varies by the number and chemical property of the substituent(s) (148−169 cm^{-1}). They found a linear relationship between the IR frequencies of either a neutral or an anion radical of 6 different 1,4-benzoquinones and their corresponding $\Sigma\sigma_p$ values, where σ_p is a Hammett substituent constant. The most probable $\Delta\nu_Q^\circ$ value was obtained from the difference betweenthe *y* intercepts of two linear trend lines. $\Delta\nu_Q^\circ$ was 159.1 cm^{-1}.[54] This value is slightly smaller than that reported in the work of Rubstov et al. (164 cm^{-1}) yet reasonable in magnitude. With this value along with the verified Q and Q^- mode CO stretching frequencies measured by the TrIR spectroscopic method, we were able to determine ξ and the corresponding H_{DA} values (Table 2). The calculated H_{DA} values for **TQ_T** and **TQ_TPh** are found to be 1600 ± 190 and 1580 ± 190 cm^{-1}, respectively (Table 2). A slightly larger H_{DA} in **TQ_T** relative to **TQ_TPh** is due to the larger ΔE.

Since $\xi \cong 2C_2^2$ and C_2 is expected to scale with the Mulliken population and thus the partial charge built on the acceptor in the ground state,[23] we calculated such values by the following equations

$$\Delta q_Q = \sum_{i \in QH_2} q_i - \sum_{j \in Q} q_j \quad (4)$$

$$q_i = Z_i - \sum_{r \in i} N_r \quad (5)$$

where q_i is the net atomic charge on atom *i*, Z_i is the atomic number of atom *i*, and N_r is the gross population. For proper evaluation, we first calculated the charge built on the hydroquinone moiety (q_i) of **TQH2_T** and **TQH_2_TPh**, where Q is replaced with hydroquinone and thus a charge resonance between **T_T** and Q is not allowed. Each atomic charge was summed over all atoms that belong to the hydroquinone moiety ($\Sigma_{i\in QH2}q_i$). We then calculated the charge built on the Q moiety (q_j) of **TQ_T** and **TQ_TPh** by the same procedure. The difference (Δq_Q) between the summed charges of QH_2 ($\Sigma_{i\in QH2}q_i$) and Q ($\Sigma_{j\in Q}q_j$) is listed in Table 2. We also listed the value calculated for the **1a_Zn** system[23] for comparison. In the ground state, the Q moieties of **TQ_T** and **TQ_TPh** are 0.078 *e* and 0.074 *e*, respectively. Q in the **1a_Zn** reference system is 0.11*e*. Given that the H_{DA} value of **1a_Zn** was reported to be 2330 cm^{-1} with 0.11*e* of Δq_Q, 0.078 *e* of Δq_Q in **TQ_T** is expected to scale 1650 cm^{-1} of H_{DA}. This result is in excellent agreement with the experimentally determined H_{DA} (~1600 cm^{-1}, Table 2). Moreover, Δq_Q in **TQ_TPh** (0.074 *e*) corresponds

dx.doi.org/10.1021/jp207122e |J. Phys. Chem. C 2011, 115, 22557–22562

Table 2. Ground (ν_Q) and CT (ν_Q^-) State CO Stretching Frequencies along with Absolute ($\Delta\nu_Q$) and Relative (ξ) Frequency Differences, Ground-State Mulliken Population of Acceptor (q_Q), and Electronic Coupling between G and CT states (H_{DA})

	ΔE^a (cm^{-1})	ν_Q (cm^{-1})	ν_Q^- (cm^{-1})	$\Delta\nu_Q$ (cm^{-1})	$\Delta\nu_Q^\circ$ (cm^{-1})	ξ (%)	$\Delta q_Q{}^b$ (e)	H_{DA} (cm^{-1})
TQ_T	9257	1661 ± 1	1511 ± 1	150 ± 2 ($\Delta\nu_1$)	159.1[c]	5.7 ± 1.3	0.078	1600 ± 190
TQ_TPh	9104	1661 ± 1	1511 ± 1	150 ± 2 ($\Delta\nu_2$)	159.1[c]	5.7 ± 1.3	0.074	1580 ± 190
1a_Zn[d]		1656	1504	152	163.7	7.3	0.110	2330

[a] See ref 26. [b] Δq_Q is the charge built on the Q moiety at the G state computed by $\Delta qQ = \Sigma_{i\in QH_2} q_{QH_2} - \Sigma_{j\in Q} q_Q$. q_A is the net atomic charge on atom A as $q_A = Z_A - \Sigma_{r\in A} N_r$, where N_r is the gross population. Therefore, $\Sigma_{i\in QH_2} q_{QH_2}$ represents the charge summed over all atoms that belong to hydroquinone moiety in **TQH$_2$_T** or **TQH$_2$_TPh** and $\Sigma_{j\in Q} q_Q$ does that belong to the Q moiety in **TQ_T** or **TQ_TPh**. [c] On the basis of the linear Hammett plot with data listed in ref 53.[54] [d] From ref 23.

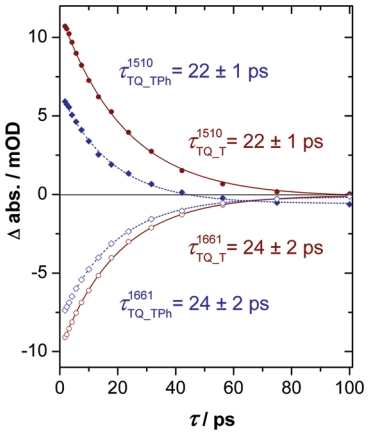

Figure 4. Decay kinetics of the Q$^-$ (top) and Q (bottom) CO stretching mode (experimental conditions: λ_{ex} = 575 nm, solvent = CD_3CN; temp =23 ± 1 °C).

to 1570 cm^{-1} of H_{DA}, which is also consistent with the experimental result (~1580 cm^{-1}, Table 2). These results clearly indicate that the TrIR spectroscopic method provides a physically acceptable H_{DA} value with a fair degree of accuracy.

In conclusion, the electronic transitions of newly constructed **TQ_T** and **TQ_TPh**, where an electron acceptor Q unit is juxtaposed cofacially with the central pyridyl ring of a tpy ligand with a typical van der Waals distance, are mainly MLCT in nature, similar to that observed in the **T_T** benchmark system, and does not exhibit a distinguishable MQCT absorption. The absence of an MQCT band can be ascribed to the lack of efficient orbital interaction between Ru-centered occupied orbitals and Q-centered unoccupied ones. TD-DFT calculation results support the observations from the experimental absorption spectra that the collective oscillator strength of the MQCT bands remains only ~0.002 for both complexes. For these particular systems, H_{DA} values between the ground and the lowest energy MQCT states, which cannot be obtained by conventional Mulliken−Hush analysis, were successfully evaluated by the TrIR spectroscopic method. The Q/Q$^-$ mode CO stretching frequency difference ($\Delta\nu_Q$) measured by this approach gives ξ = ~5.7% for both **TQ_T** and **TQ_TPh**, which corresponds to the ground−MQCT H_{DA} of 1600 ± 190 and 1580 ± 190 cm^{-1}, respectively. These values are in excellent agreement with those evaluated separately by Mulliken population analysis. This work demonstrates that the TrIR spectroscopic method can be a useful tool for evaluation of G−CT H_{DA} where a CT absorption band is not available.

■ ASSOCIATED CONTENT

Supporting Information. Experimental section, synthetic scheme, table of calculated CT state wave functions, time-resolved TrIR spectra, and 1D- and 2D-NMR data. This material is available free of charge via the Internet at http://pubs.acs.org.

■ AUTHOR INFORMATION

Corresponding Author

*E-mail: mhlim@pusan.ac.kr (M.L.); ykchung@snu.ac.kr (Y.K.C.); younkang@smu.ac.kr (Y.K.K.).

■ ACKNOWLEDGMENT

This work was supported by the Basic Science Research Program through the National Research Foundation of Korea funded by the Ministry of Education, Science and Technology (2011-0004014, 2010-0029663, and 2011-0016114). H.M.K., J. P., and Y.T.L. thank the Brain Korea 21 fellowships and the Seoul Science Fellowships.

■ REFERENCES

(1) Mulliken, R. S. *J. Am. Chem. Soc.* **1952**, *74*, 811–824.
(2) Hush, N. S. *Prog. Inorg. Chem.* **1967**, *8*, 391–444.
(3) Sutin, N. *Prog. Inorg. Chem.* **1983**, *30*, 441–498.
(4) Creutz, C.; Newton, M. D.; Sutin, N. *J. Photochem. Photobiol., A: Chem.* **1994**, *82*, 47–59.
(5) Brunschwig, B. S.; Creutz, C.; Sutin, N. *Chem. Soc. Rev.* **2002**, *31*, 168–184.
(6) Demadis, K. D.; Hartshorn, C. M.; Meyer, T. J. *Chem. Rev.* **2001**, *101*, 2655–2685.
(7) Sauvage, J. P.; Collin, J. P.; Chambron, J. C.; Guillerez, S.; Coudret, C.; Balzani, V.; Barigelletti, F.; Decola, L.; Flamigni, L. *Chem. Rev.* **1994**, *94*, 993–1019.
(8) Newton, M. D. *Chem. Rev.* **1991**, *91*, 767–792.
(9) Richardson, D. E.; Taube, H. *Coord. Chem. Rev.* **1984**, *60*, 107–129.
(10) Creutz, C. *Prog. Inorg. Chem.* **1983**, *30*, 1–73.
(11) Sun, D.; Rosokha, S. V.; Kochi, J. K. *J. Am. Chem. Soc.* **2004**, *126*, 1388–1401.
(12) Bailey, S. E.; Zink, J. I.; Nelsen, S. F. *J. Am. Chem. Soc.* **2003**, *125*, 5939–5947.
(13) Cooley, L. F.; Han, H.; Zimmt, M. B. *J. Phys. Chem. A* **2002**, *106*, 884–892.
(14) Bixon, M.; Jortner, J.; Verhoeven, J. W. *J. Am. Chem. Soc.* **1994**, *116*, 7349–7355.
(15) Gould, I. R.; Young, R. H.; Mueller, L. J.; Albrecht, A. C.; Farid, S. *J. Am. Chem. Soc.* **1994**, *116*, 3147–3148.
(16) Reimers, J. R.; Hush, N. S. *Inorg. Chem.* **1990**, *29*, 3686–3697.

(17) Oevering, H.; Verhoeven, J. W.; Paddonrow, M. N.; Warman, J. M. *Tetrahedron* **1989**, *45*, 4751–4766.
(18) Desbois, M. H.; Astruc, D.; Guillin, J.; Mariot, J. P.; Varret, F. *J. Am. Chem. Soc.* **1985**, *107*, 5280–5282.
(19) Cave, R. J.; Newton, M. D. *Chem. Phys. Lett.* **1996**, *249*, 15–19.
(20) Cave, R. J.; Newton, M. D. *J. Chem. Phys.* **1997**, *106*, 9213–9226.
(21) Zheng, J. R.; Kang, Y. K.; Therien, M. J.; Beratan, D. N. *J. Am. Chem. Soc.* **2005**, *127*, 11303–11310.
(22) Voityuk, A. A. *Chem. Phys. Lett.* **2006**, *422*, 15–19.
(23) Rubtsov, I. V.; Kang, Y. K.; Redmore, N. P.; Allen, R. M.; Zheng, J. R.; Beratan, D. N.; Therien, M. J. *J. Am. Chem. Soc.* **2004**, *126*, 5022–5023.
(24) In this two-state model, the overlap integral S is neglected.
(25) $\Delta\nu_Q^\circ = \nu_Q^\circ - \nu_{Q^-}^\circ$, where ν_Q° and $\nu_{Q^-}^\circ$ are diabatic ground and CT state CO frequencies, respectively. Similarly, $\Delta\nu_Q = \nu_Q - \nu_{Q^-}$, where ν_Q and ν_{Q^-} are the corresponding adiabatic parameters.
(26) Calculated by the equation $\Delta E = e(E_{red} - E_{ox}) + \frac{e^2}{4\pi\varepsilon_0\varepsilon_S R_{DA}}$, where E_{red} and E_{ox} are the respective acceptor (Q) and donor ($[Ru(tpy)_2]^{2+}$) redox potentials, ε_s is the solvent dielectric constant, and R_{DA} is the Ru-to-quinonyl centroid distance.
(27) Creutz, C.; Brunschwig, B. S.; Sutin, N. *J. Phys. Chem. B* **2005**, *109*, 10251–10260.
(28) Creutz, C.; Brunschwig, B. S.; Sutin, N. *Chem. Phys.* **2006**, *324*, 244–258.
(29) Creutz, C.; Brunschwig, B. S.; Sutin, N. *J. Phys. Chem. B* **2006**, *110*, 25181–25190.
(30) Heuberger, B. D.; Shin, D.; Switzer, C. *Org. Lett.* **2008**, *10*, 1091–1094.
(31) Sullivan, B. P.; Calvert, J. M.; Meyer, T. J. *Inorg. Chem.* **1980**, *19*, 1404–1407.
(32) Taher, D.; Thibault, M. E.; Di Monde, D.; Schlaf, M. *Chem.—Eur. J.* **2009**, *15*, 10132–10143.
(33) Aleman, E. A.; Shreiner, C. D.; Rajesh, C. S.; Smith, T.; Garrison, S. A.; Modarelli, D. A. *Dalton Trans.* **2009**, 6562–6577.
(34) Kim, J.; Park, J.; Lee, T.; Lim, M. *J. Phys.Chem.B.* **2009**, *113*, 260–266.
(35) Lee, T.; Park, J.; Kim, J.; Joo, S.; Lim, M. *Bull. Korean Chem. Soc.* **2009**, *30*, 177–182.
(36) Kim, S.; Jin, G.; Lim, M. *J. Phys.Chem.B.* **2004**, *108*, 20366–20375.
(37) Frisch, M. J. *Gaussian 09*, Revision B.01; Gaussian, Inc.: Wallingford, CT, 2010.
(38) Kohn, W.; Sham, L. J. *Phys. Rev.* **1965**, *140*, A1133–A1138.
(39) Becke, A. D. *J. Chem. Phys.* **1993**, *98*, 5648–5652.
(40) Stephens, P. J.; Devlin, F. J.; Chabalowski, C. F.; Frisch, M. J. *J. Phys. Chem.* **1994**, *98*, 11623–11627.
(41) Hertwig, R. H.; Koch, W. *Chem. Phys. Lett.* **1997**, *268*, 345–351.
(42) Pietro, W. J.; Francl, M. M.; Hehre, W. J.; DeFrees, D. J.; Pople, J. A. *J. Am. Chem. Soc.* **1982**, *104*, 5039–5048.
(43) Lee, C. T.; Yang, W. T.; Parr, R. G. *Phys. Rev. B* **1988**, *37*, 785–789.
(44) Hay, P. J.; Wadt, W. R. *J. Chem. Phys.* **1985**, *82*, 270–283.
(45) Wadt, W. R.; Hay, P. J. *J. Chem. Phys.* **1985**, *82*, 284–298.
(46) Hay, P. J.; Wadt, W. R. *J. Chem. Phys.* **1985**, *82*, 299–310.
(47) Hehre, W. J.; Ditchfield, R.; Pople, J. A. *J. Chem. Phys.* **1972**, *56*, 2257–2261.
(48) Runge, E.; Gross, E. K. U. *Phys. Rev. Lett.* **1984**, *52*, 997–1000.
(49) Bartolotti, L. J. *Phys. Rev. A* **1982**, *26*, 2243–2244.
(50) Iovine, P. M.; Kellett, M. A.; Redmore, N. P.; Therien, M. J. *J. Am. Chem. Soc.* **2000**, *122*, 8717–8727.
(51) Iovine, P. M.; Veglia, G.; Furst, G.; Therien, M. J. *J. Am. Chem. Soc.* **2001**, *123*, 5668–5679.
(52) All electrochemical potentials are relative to NHE.
(53) Clark, B. R.; Evans, D. H. *J. Electroanal. Chem.* **1976**, *69*, 181–194.
(54) They reported the average value was 155 cm^{-1}. However, the value has been modified to 159.1 cm^{-1}, while we reproduced the plot with data listed in their paper.